



www.editada.org

## Autonomous Robotic Platform for Germicidal Disinfection and Air Purification Using UVC and Nebulization Technology

Griselda Cortés Barrera<sup>1,2</sup>, Adolfo Meléndez Ramírez<sup>1,4</sup>, Francisco Jacob Ávila Camacho<sup>1,4</sup>, Ernesto Enciso Contreras<sup>1,2</sup>, Mishel Enrique Brito Herrera<sup>2</sup>, Sergio Viguera Carmona<sup>1</sup>, Humberto Sossa Azuela<sup>3</sup>

<sup>1</sup>Tecnológico Nacional de México/TESE. Ecatepec, Estado de México.

<sup>2</sup>Laboratorio Nacional Conahcyt en Inteligencia Artificial y Ciencia de Datos (LNC-IACD). Ecatepec, Estado de México.

<sup>3</sup>Instituto Politécnico Nacional, Centro de Investigación en Computación, México.

<sup>4</sup>Centro de Cooperación Academia Industria - TESE . Ecatepec, Estado de México.

E-mails: gortes@tese.edu.mx, adolfo\_melendez@tese.edu.mx, fjacobavila@tese.edu.mx, sviguera@tese.edu.mx, ernesto\_contreras@tese.edu.mx, humbertosossa@gmail.com

**Abstract.** This work presents an autonomous robotic platform aimed at improving indoor air quality and ensuring effective disinfection. The system leverages UVC germicidal radiation and a nebulization module to eliminate pollutants, including ozone and microbial pathogens, aligning with Sustainable Development Goals (SDGs) 3 and 11. The robotic platform incorporates six 253.7 nm UVC lamps arranged to maximize disinfection efficiency, achieving 95% microbial reduction within 14.76 seconds for irradiated areas of 0.98–1.04 m<sup>2</sup>. An integrated olfactory system, using MQ-131 and MQ-135 sensors, monitors ozone and CO<sub>2</sub> concentrations, ensuring environmental safety by automatically shutting down disinfection processes when thresholds are exceeded. The nebulization system disperses a hydrogen peroxide (H<sub>2</sub>O<sub>2</sub>) solution, reducing ozone levels from 29.22 ppm to 0.05 ppm in enclosed spaces within 3 seconds.

The experimental results demonstrate the platform's capability to sanitize surfaces, walls, floors, and ceilings in diverse indoor environments, such as hospitals and classrooms, with minimal human intervention. By combining tele controlled and autonomous functionalities, the system offers a scalable solution for sustainable and inclusive urban environments, addressing key challenges in air quality and health resilience post-COVID-19. This innovation contributes significantly to the goals of creating healthier living spaces and advancing the development of smart, sustainable cities.

**Keywords:** Tropospheric Ozone Control, Airborne Ozone Degradation, Indoor Air Quality Improvement, Air Purification System, Atmospheric Pollutant Elimination.

Article Info

Received Jan 26, 2025

Accepted Mar 11, 2025

## 1 Introduction

The 2030 Agenda for Sustainable Development aims to tackle urgent global challenges, but the COVID-19 pandemic has intensified existing crises, revealing public health and environmental shortcomings. The 2020 SDG Report highlights ongoing environmental degradation and the insufficiency of large-scale changes. Among the issues raised, indoor ozone pollution poses a serious health risk, stemming from sources such as industrial processes and household appliances.

The COVID-19 pandemic has exposed the significant limitations of current systems in ensuring disinfection and air quality in indoor spaces, leading to an unprecedented health crisis. This situation underscores the urgent need to implement efficient and sustainable technologies to reduce the spread of pathogens and improve environmental conditions in enclosed spaces such as hospitals, offices, and homes. Additionally, contaminants like tropospheric ozone, which accumulate indoors due to natural sources and human activities, exacerbate public health risks, causing respiratory illnesses and material damage [1, 2, 3].

Controlling ozone and other indoor contaminants necessitates innovative solutions that integrate detection, disinfection, and neutralization technologies. Despite advancements in air purifiers and filtration systems, these technologies still face limitations in scope, efficiency, and sustainability. Therefore, there is a pressing need to develop integrated and autonomous platforms that combine multiple approaches to comprehensively address this challenge [1, 4, 5, 6, 7, 8, 9].

In this context, this work introduces an autonomous robotic platform designed for germicidal disinfection and air purification in indoor spaces. The system employs 253.7 nm germicidal UVC radiation and a nebulization module to eliminate microorganisms and reduce ozone concentrations in the environment. Additionally, the integration of an olfactory system based on MQ-131 and MQ-135 sensors enables real-time monitoring of atmospheric contaminants, ensuring operational safety and minimizing environmental impact. This development aligns with Sustainable Development Goals (SDGs) 3 and 11, which aim to ensure health and well-being and promote sustainable and inclusive cities [10].

The primary objective of this research is to demonstrate the efficacy of the robotic platform in improving indoor air quality and surface disinfection by evaluating its performance under controlled conditions. Through experimental tests, we will analyze optimal disinfection times, microorganism elimination efficiency, and ozone reduction capacity via nebulization. The results obtained will provide a framework for future applications in environments such as hospitals, schools, and other critical spaces, thereby contributing to health resilience and a healthier, more sustainable environment.

## 2 Related works

The implementation of autonomous disinfection robots utilizing ultraviolet C (UV-C) light has proven to be a highly effective and safe solution for the elimination of pathogenic microorganisms in various environments. These robots not only increase the efficiency of disinfection processes by significantly reducing the time required to sanitize surfaces and spaces but also eliminate the need for toxic chemicals. Furthermore, their autonomous operation minimizes staff exposure to potential contaminants, thereby increasing safety in hospitals, offices, and other public areas. In conclusion, this technology represents a significant advancement in the prevention of disease transmission, providing a powerful tool for maintaining cleaner and safer environments [11, 12].

Recent analyses of various air purification technologies have evaluated their effectiveness and applicability. These technologies include HEPA (High Efficiency Particulate Air) filtration, which removes up to 99.97% of particles 0.3 microns or larger; bipolar ionization, which generates ions to neutralize contaminants and is effective against particles, bacteria, and viruses; photocatalytic oxidation, which uses a UV light-activated photocatalyst to break down volatile organic compounds (VOCs) and microorganisms; and ultraviolet light (UV-C), which inactivates pathogenic microorganisms and is ideal for disinfecting surfaces and air. Each technology has specific advantages depending on the contaminant type and environment, which emphasizes the necessity of combining multiple technologies for more complete and effective air purification [13], [14].

The oxidation processes, which include ozone ( $O_3$ ), ozone with hydrogen peroxide ( $O_3/H_2O_2$ ), and ultraviolet light with hydrogen peroxide (UV/ $H_2O_2$ ), are considered effective for disinfection [15, 16].

The literature emphasizes innovative technologies engineered to enhance indoor air quality, including systems based on electrostatic spraying, which utilize electrically charged aerosols to efficiently remove contaminants without producing ozone or causing pressure drops. Additional approaches propose integrated solutions that combine HEPA filtration, activated carbon adsorption, and ultraviolet (UV) light to eliminate particles, toxic gases, and microorganisms. These systems incorporate sensors to monitor key air parameters such as temperature, humidity, particulate matter, and volatile compounds, significantly improving air purification and promoting the well-being of occupants in enclosed spaces [17,18].

Airborne Ozone Degradation, which neutralizes ozone in indoor air to ensure safer environments, is a crucial process. Ozone, a health hazard at high concentrations, is often produced by UVC disinfection systems. Advanced solutions, such as hydrogen peroxide ( $H_2O_2$ ) nebulization and real-time monitoring with sensors (e.g., MQ-131, MQ-135), can effectively reduce ozone levels. The integration of these technologies into autonomous robotic platforms enhances disinfection efficiency, improves air quality, and minimizes environmental impact, thereby aligning with global sustainability and health goals.

The literature shows that technologies such as UVC radiation are highly effective for inactivating pathogenic microorganisms on surfaces and in the air. However, these technologies face challenges related to coverage, energy efficiency, and potential side effects, such as ozone generation. For instance, recent studies have reported disinfection efficiencies of up to 98% in small

spaces using configurations of multiple UVC lamps; however, this was achieved with prolonged exposure times and without the integration of ozone mitigation systems.

Meanwhile, complementary technologies like hydrogen peroxide ( $H_2O_2$ ) nebulization have proven effective in reducing indoor ozone concentrations and significantly improving air quality. Nonetheless, the integration of these technologies with autonomous systems and real-time sensors remains an area of development, which limits their large-scale practical application. Contemporary advancements in the mitigation of indoor air pollution emphasize the utilization of both active and passive ozone control technologies, coupled with the integration of sophisticated hydroxyl radical (OH)-based systems [19, 20].

In this context, we propose an autonomous robotic platform that combines UVC radiation with an  $H_2O_2$  nebulization system and an integrated olfactory system for monitoring and mitigating atmospheric contaminants. This solution not only addresses current challenges in disinfection and air purification but also optimizes energy and resource usage by automatically deactivating systems when safe contaminant levels are reached. Additionally, its modular design and autonomous operation capabilities make it a scalable and adaptable tool for various environments.

Autonomous robotic platforms that combine Airborne Ozone Degradation technologies, such as nebulization with UVC germicidal lamps, not only enhance the overall efficiency of disinfection processes but also ensure minimal environmental impact and improved indoor air quality. This integration directly supports health resilience and aligns with global efforts to create safer, more sustainable urban environments.

### 3 Proposed architecture

To advance the 2030 Agenda for Sustainable Development's SDG3 and SDG11, reduce infections among citizens, diminish air pollution and health concerns, and bolster resilience to health crises, this article presents a robotic platform for sanitizing spaces. The platform features UV-C light, remote control and autonomous operation, and a system to measure tropospheric ozone levels emitted by UVC lamps in the work environment, automatically deactivating the lamps when necessary.

Version 2.0 of the robotic platform integrates an electronic nose to detect ozone levels and a nebulizer with hydrogen peroxide to reduce ozone concentration.

#### 3.1 Structural architectural module

The design of an electromechanical, kinematic mobile robotic platform with differential tracing, is described below.

- a) Fig. 1a shows the mechanical structure of clamping and mounting the traction, power, control, UVC lamps, telemetry, communication module and robot cover. It is composed of an aluminum square tubular profile of 1 3/4" for support posts and frames of 1 1/4" and 3/8" thick aluminum plate.
- b) The powertrain consists of two servo motors of 250w, 141.73mm, 24-75v and 3950 rpm, 2 rear neoprene wheels of 6". To control speed and increase tire torque, use speed reducers (2x38mm pulleys and 2x100mm pulleys with toothed belts, and two 100 mm outer diameter pulleys, one of the latter will be concentric to each rear wheel where the final movement will be made, see Fig. 1b).

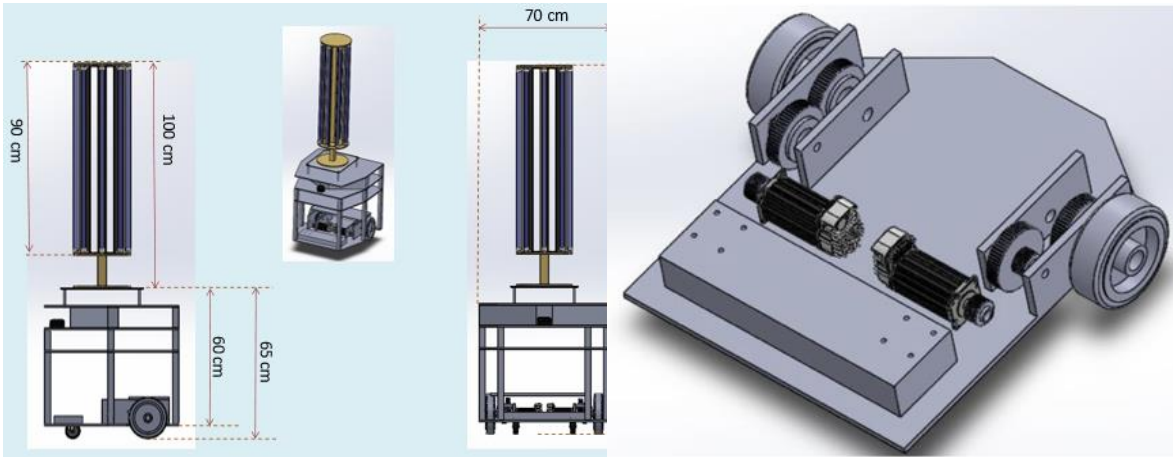


Fig. 1 a) Design of the robot, b) Powertrain control module

- c) for steering eq. (1) and (2) is used, corresponding to the model of the speed system by the speeds difference  $v_1$  and  $v_2$ . This system is very useful if we consider the possibility of changing its orientation without translational movement.

$$V = R \frac{v_2 + v_1}{2} = R \frac{\omega_2 + \omega_1}{2}, \quad (1)$$

$$\omega = R \frac{v_2 - v_1}{L} = R \frac{\omega_2 + \omega_1}{L}$$

where  $V$  is the linear speed of the mobile robot,  $v_1$  is the speed of the left wheel,  $v_2$  is the speed of the right wheel,  $R$  the radius of both wheels, and  $L$  the length that separates them. The dynamic model that defines the differential robot is obtained, given by eq. (1), and (3).

$$\dot{x} = V \cos \theta, \quad \dot{y} = V \sin \theta, \quad \dot{\theta} = \omega \quad (2)$$

that is expressed by his Jacobian model thus:

$$\begin{bmatrix} \dot{x}' \\ \dot{y}' \\ \dot{\theta}' \end{bmatrix} = \begin{bmatrix} \cos \theta & 0 \\ \sin \theta & 0 \\ 0 & 1 \end{bmatrix} \cdot \begin{bmatrix} V \\ \omega \end{bmatrix} \quad (3)$$

The traction system has an independent Li-ion power system. The battery was assembled with lithium-ion cells; each cell has a nominal voltage of 3.7V and a maximum voltage of 4.2V. The storage capacity of each cell is 3000 mA. The robot requires 13 batteries in series, which provides a total of 48.1V, or 54.6V when charged to maximum capacity. Furthermore, 40 cells were arranged in parallel to provide a total of 120 amperes, or the equivalent of 120,000 mA.

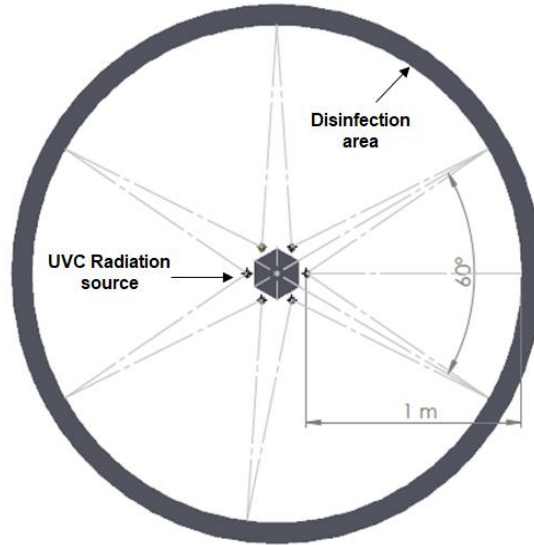


Fig. 2 Top view of UVC radiation.

### 3.2 UVC Energy Efficiency Module

It has been shown that the family of Coronaviruses in general are very sensitive to ultraviolet radiation at different wavelengths (**200 nm - 360 nm**). Some scholarly articles have demonstrated the use of UVC for water treatment [21], Pulmonary Infections [22], [23], Air and Surface Treatment [24]. The robot has low-pressure mercury germicidal 6 lamps with short wave **253.7 nm** and **30 w**.

**Error! Reference source not found.** and **Error! Reference source not found.**, show the design of the configuration of the robot's UVC radiation system: a) 6 vertical lamps at the top, each pointing towards a cardinal point, in such a way that the light is projected radially.

The efficacy of UVC sanitation is primarily dependent on the dose administered to the microorganisms  $J/m^2$  [23], [24]. However, it is complex to determine the sanitization efficiency, this will depend on the direction of ultraviolet radiation, the survival fraction of microorganisms that have been exposed to UVC radiation and the resistance to inactivation of each species. In general, when exposed to light, microorganisms show susceptibility. **Error! Reference source not found.**, allows to calculate the radiation coverage of UVC lamps, thus.

$$C = 2\pi d, \quad a(\theta)_i = \theta * R, \quad e_w = \frac{x}{a} \tag{4}$$

where  $C$  represents the perimeter,  $d$  the distance,  $a$  the irradiated area,  $\theta$  ( $rad$ ) the central angle,  $R$  the radius,  $e$  radiated energy,  $w$  Lamp power at 95%,  $x$  is the energy produced in  $J/s$ .

To evaluate the time of disinfection considering results of [25] and the equation

$$t = \frac{en}{e_w} \tag{5}$$

where  $t$  represents the disinfection seconds required,  $en$  is the energy necessary and  $e_w$  is the energy radiated to deactivate microorganism and  $w$  is the 95% lamps radiation potency

The subsystems that will allow to identify the electronic components that give functionality to the UVC sanitizer robot with automatic and sustainable system are described below (Fig. 3).

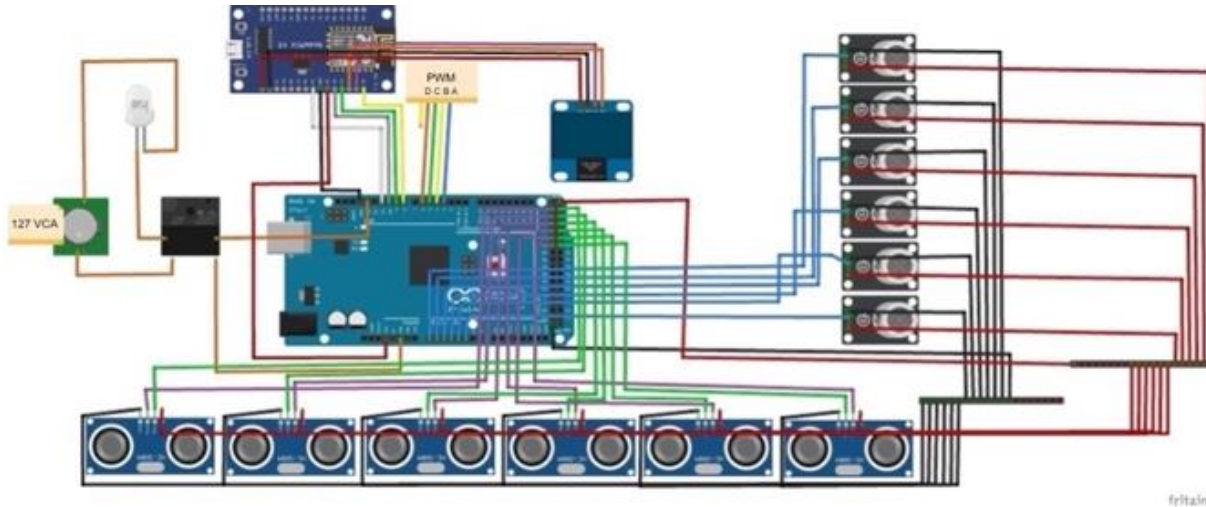


Fig. 3 Circuit of the Robot Remote Control Module.

### 3.2.1 Remote operation

The electronic components to control the robot remotely are: a) an IP camera with MJPEG format for navigation vision, b) at least one Access Point to establish bidirectional communication through web sockets and transmission of http streams, c) a Node-MCU-ESP8266 Microcontroller with integrated 2.4GHz WiFi, operated at 32 bits: allows asynchronous communication capable of receiving instructions from the mobile application to transform them into electrical impulses than the ATMEGA2560. It will be able to receive and transform into PWM signals for the control of motors, adding a relay of 5 -12 V that will allow the passage of current (110V-120V) to drive lamps. To avoid a collision with walls or objects, 6 ultrasonic sensors were integrated to measure the maximum distance (25cm) and send a pulse to stop the robot.

Table 1 ATmega2560 and NodeMCU connections

No.	Pin	Action
13	Ánodo	Output-energy efficiency(lamps)
22-32	Trigger/Echo	Ultrasonic sensor
A0-A6	Analog In	MQ sensor
5	R_PWM	Signals PWM
4	L_PMW	Signals PWM
3	L_EN	VCC
2	E_EN	VCC
22	D0	MCU Binary instruction 2 <sup>3</sup>
24	D1	MCU Binary instruction 2 <sup>3</sup>
26	D2	MCU Binary instruction 2 <sup>3</sup>
28	D5	MCU I/O de Lamps (Send 0/1)
	Neuter	Inverter 110-120v
	Relay 5-12V	

Table 1 shows the connection of the pins of the microcontrollers. From the app, commands AT are sent for the remote displacement of the robot (stop, advance, backwards, turn left and right), pins D0, D1 and D2 are configured NodeMCU with a

binary value (23); pin D5 for the lamps is also sat (**Error! Reference source not found.a y Error! Reference source not found.**).

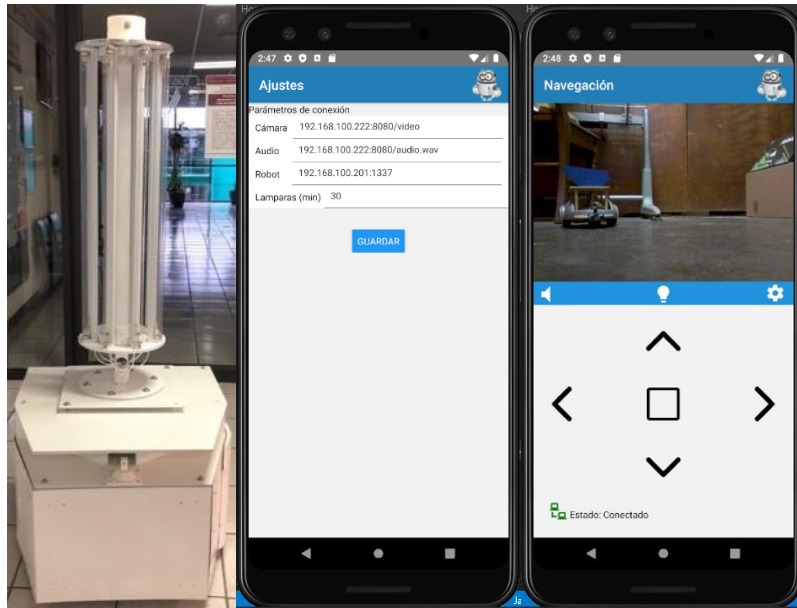


Fig. 4 a) Germicidal robot with electronic nose and nebulizer system, b) mobile app

### 3.2.2 Mobile application to remote control

To establish two-way Wi-Fi communication between the application and the robot remotely, the "Generic ESP8266 Module" board had to be configured using the Arduino IDE. This involved downloading and adding the WebSockets and ESPAsyncTCP libraries in Arduino. Subsequently, the ControlRobot.ino code was uploaded to the board. The \*ssid and \*password variables were set for automatic connection with the access point, and an IP address and port were assigned. The IP camera, which transmits in MJPEG format via real-time streaming, enables the visualization of the robot's navigation from the mobile application, see Fig. 4b.

### 3.2.3 Olfactory System

This system has two functions: a) Automatic and sustainable disinfection: and b) Embedded system for concentration of chemicals absorbed into the environment. The robot has a camera (Fig. 5) inside the telemetry module (Fig. 3) and through a fan allows it to capture the ozone concentration and other gases that exist in the air. The goal is to automatically disable the disinfection system and obtain the characteristic patterns of the environment to identify the level of pollution.

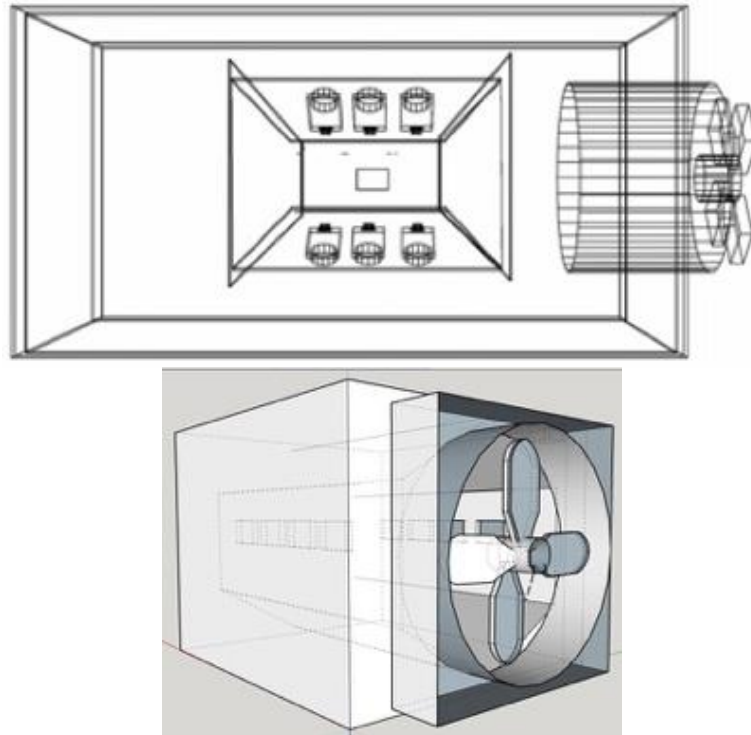


Fig. 5 Gas concentrator chamber O<sub>3</sub> y CO<sub>2</sub>

### 3.2.4 Olfactory System

This system has two functions: a) Automatic and sustainable disinfection: and b) Embedded system for concentration of chemicals absorbed into the environment. The robot has a camera (Fig. 5) inside the telemetry module (Fig. 3) and through a fan allows it to capture the ozone concentration and other gases that exist in the air. The goal is to automatically disable the disinfection system and obtain the characteristic patterns of the environment to identify the level of pollution.

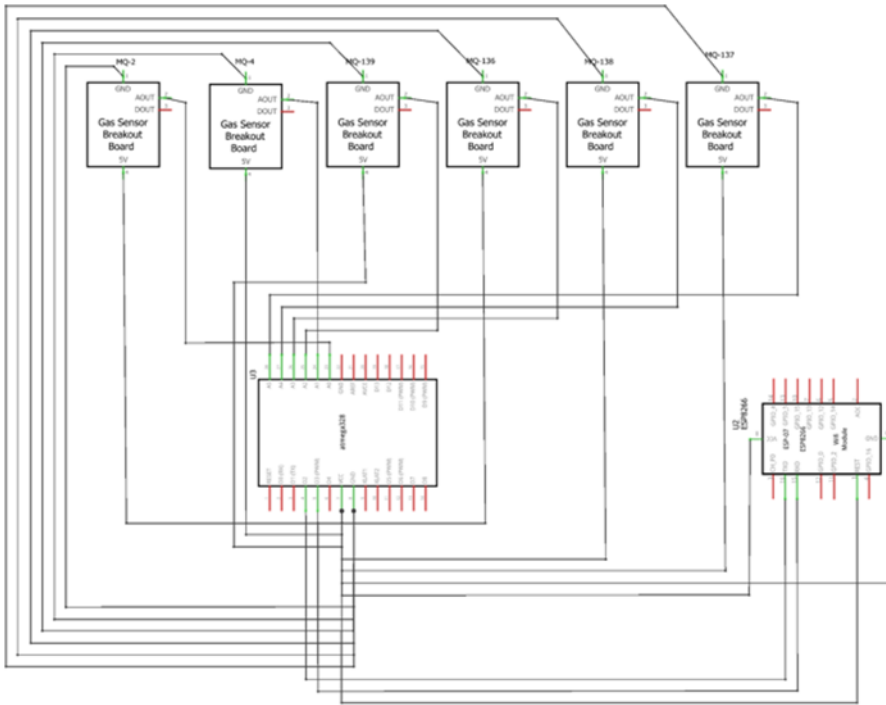


Fig. 6 Diagrama de conexión del módulo de R/W inalámbrica.

The Embedded System of the Atmosphere Pattern Concentrator Chamber has a system for acquiring and collecting data read by the sensors, see Fig. 6. To achieve this, the following is done:

**Server Configuration:** for configuration and communication with the Wi-Fi module, the microcontroller is programmed ESP8266 via the Arduino IDE. To send and receive data over a wireless network, the ESP-01 module is configured using the SoftwareSerial.h library to indicate that pin 2 will be used as the TX endpoint and pin 3 as the RX.

Considering that the communication with the MQ-135 to measure air quality (CO<sub>2</sub>) and MQ-131 to detect ozone (O<sub>3</sub>) sensors will be through I2C, it will require 5V power, and the GPIO pins of the

ESP8266 will be powered at 3.3V. To address this, an MB-102 power supply will be used. The MQ-135 sensor has an estimated lifespan of around 2 years under continuous use <https://docs.cirkitdesigner.com/component/17438be0-fe02-4360-aeab-7e4a5c6dd4cc/mq135>, the MQ-131 sensor typically lasts for several years with proper maintenance regular calibration and maintenance are recommended to ensure accurate and reliable performance over time

<https://docs.cirkitdesigner.com/component/9dfbd613-67f0-4abc-a85e-181acb22cc54/mq-131-sensor-ozone-gas>.

To configure the sensors (MQ-135 and MQ-131) and install libraries with Arduino IDE to send data through Websokets in real time, see <https://www.arduino.cc/reference/en/libraries>.

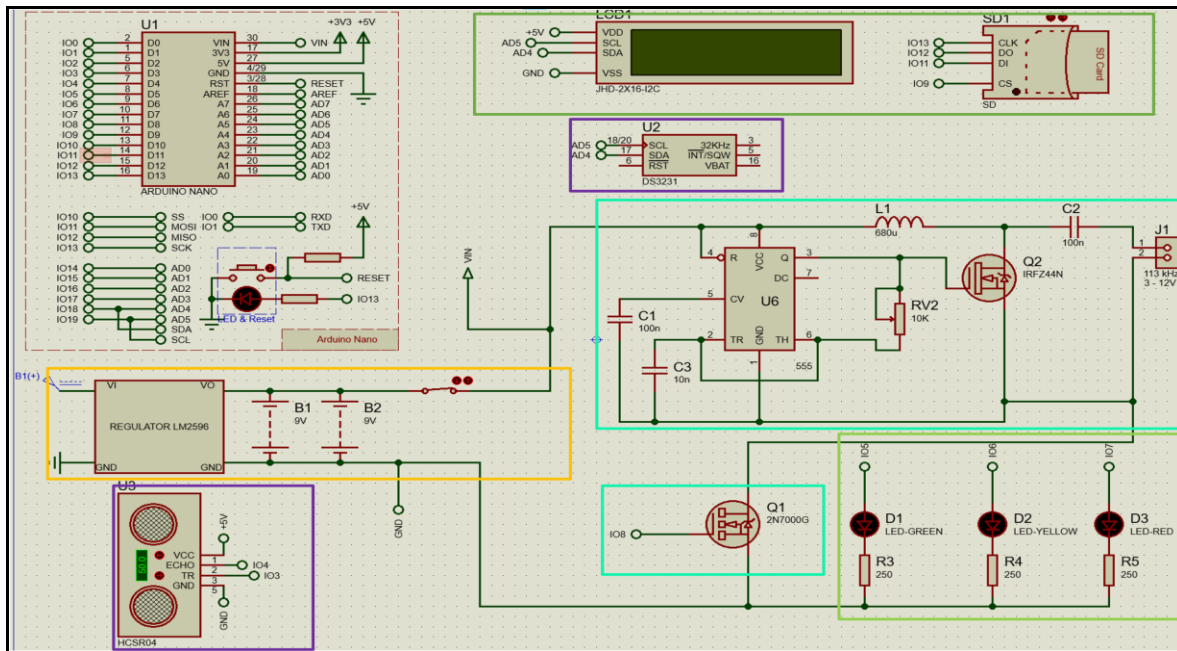


Fig. 7 Nebulizer system diagram

### 3.2.5 Nebulizer system

To clear the atmosphere. La Fig. 7 shows the Embedded System nebulizer Diagram. This architecture has 4 modules and described below:

- a) Power regulation: ensures the functionality, stability and safety of the microcontroller (nano arduino), using a voltage conversion regulator (LM2596), a 9V battery to supply power to the general circuit.
- b) Nebulizer system: Requires a timer TLC555, inductor 680u, Timmer 10k, transistor IRFZ44N, ceramic capacitors of 100nF y 10nF, and piezoelectric of 113kHz to convert the liquid in the container into microdroplets.

- a) *Liquid Monitoring*: Controls the misting system using an ultrasonic sensor and module DS3231.
- b) *Data Output*: Locally monitors device operation via an *LCD-I2C*, and an LED traffic light to measure the liquid level, the operation data such as: liquid quantity, date and time, status and lifetime) are stored in a *datalogger* in *txt* format.

### 3.3 Protocol to measure disinfection efficiency

Below we list the protocol for measuring air quality and clear atmosphere at enclosed space is:

- a) Calibrate the olfactory system.
- b) Pour the solution H<sub>2</sub>O<sub>2</sub> into the nebulizer container.
- c) Generate ozone (Start robot disinfection process with UVC)
- d) Measure the ozone concentration in the enclosed space.
- e) Activate the nebulizer system or ventilate enclosed space.
- f) Remeasure the ozone level in the enclosed space.

### 3.4 Preparing the inoculum Salmonella

We obtained this by isolating a sample of leachate obtained from the composting of municipal organic solid waste. Once the sample was taken, enrichment was carried out by placing 4g of total solids in 36mL of tetrathionate broth, mixing for 3 minutes at 800 rpm and then incubating for 22h at 37°C.

After the enrichment time, decimal dilutions were prepared to inoculate tubes with 10 mL of cystine selenite broth with 1 mL, the already inoculated tubes are incubated for 24-72 h at 41 °C. After that time, the positive tubes (bright orange) were used for

isolation and identification. The microorganisms in the positive tubes were seeded by roasting on bright green agar and incubated, red or pink colonies surrounded by red half are listed as suspicious to be Salmonella.

For biochemistry, two well-isolated and overgrown colonies were selected. In nutritive agar, two tubes are inoculated: a) Triple Sugar and Iron agar (TSI), and b) Lysine Iron Agar (LIA) by striation on the inclined surface and by pitting on the bottom. After incubation, positive colonies react thus.

- a) *Agar TSI*: At the bottom of the tube there is a yellow color due to the fermentation of glucose, on the surface of the medium the red color intensifies. In most cases, black coloration is observed throughout the bite, due to the production of H<sub>2</sub>S.
- b) *Agar LIA*: Purple coloration is seen throughout the tube, H<sub>2</sub>S production is sometimes observed with blackening along the bite.

To prepare inoculum, a preserved strain is used by suspending in a phosphate buffer and sowing by striation on bright green agar. Once the colony is grown, 3 roasts are resuspended in 10 mL of phosphate buffer to obtain the dilution of 10<sup>0</sup>. Para las pruebas de desinfección se utilizan las cajas petri con 50 ± 5 colonias. Then, stored in Eppendorf tubes with nutrient agar and a layer of glycerol for preservation at -20 °C. The *phosphate buffer* is prepared by adding 1.25 mL of a solution of 34 g/L of KH<sub>2</sub>PO<sub>4</sub>, and 5 mL of a solution of 38.1 g/L of MgCl<sub>2</sub>·6H<sub>2</sub>O in distilled water and volumetric to 1 liter.

To evaluate the percentage of disinfection efficiency, the microbial density will be measured using the regression model eq. (6).

$$Ef_i = 77.5 + (0.0856 * t) + (14.8 * d) - (0.00731 * t^2) - (12.94 * d^2) \quad (6)$$

where,  $Ef$  represents the percentage of efficiency,  $t$  is time in minutes,  $i$  the samples total and  $d$  is the distance in  $m^2$ .

## 4 Results

This section details the experimental results obtained with the autonomous robotic platform for air disinfection and purification. It describes the disinfection efficiency, the optimal time required, and the percentage of microbial elimination achieved, highlighting the performance of the UVC system and the hydrogen peroxide nebulizer. Additionally, it includes calibration tests for the olfactory system to measure real-time pollutants and evaluates the nebulizer's capability to reduce ozone in enclosed spaces.

### 4.1. Disinfection time and radiated energy

Disinfection efficiency was evaluated using eq. (4) calculating the average energy radiated over  $m^2$  between each 253.7 nm UV cylindrical lamp and the surface, considering  $d = 1m^2$ ,  $a(60^\circ)_i = 1.04 \text{ rad}/m^2$  y  $x = 5 \text{ J}/s$ . If 95% of the total power reaches the optimal wavelength, the lamps will deliver 28.5W of germicidal power, therefore,  $e_{28.5} = 4.5382 \text{ W}/m^2$ .

To calculate the optimal disinfection time we used eq. (5), considering the average of the results of [25], we have  $en = 67 \text{ W}/m^2$ , if the lamps power are 30w, then  $e_{28.5} = 4.5382 \text{ W}/m^2$  then  $t = 14.763s$ .

### 4.2. Time and disinfection efficiency

To contrast the area of irrigation and disinfection efficiency was through the method of the upward slope. In the Anaerobic Technology Laboratory of the Tecnológico de Estudios Superiores de Ecatepec (TESE) in Mexico, the efficiency of disinfection by microbial density is tested for optimization.

The microorganisms used are salmonella coliforms, obtained and generated during the composting of fruits and vegetables. Samples contain colonies grown on bright green agar, with 24 hours incubation and will be exposed to UVC radiation  $20 \pm 5$ . After the exposure time,  $j = 3$ . Samples were randomly chosen and suspended in phosphate buffer (dilution  $10^0$ ) to prepare dilutions  $10^{-1}$ ,  $10^{-2}$  y  $10^{-3}$ .

The microorganism used is representative of the microorganisms that frequently occur in the evaluated areas. It is common to use only one reference species in this type of work [26].

Once the exposure time had elapsed, three random colonies were suspended in phosphate buffer (100 dilution) to prepare dilutions of  $10^{-5}$ ,  $10^{-6}$  and  $10^{-7}$  from here, for subsequent inoculation in boxes. Petri with bright green agar using the dispersion

technique with glass beads. They are incubated at 35 °C for 72 h and the colony forming units CFU/mL is determined, see **Error! Reference source not found.**



Fig. 8 Preparing the Salmonella inoculum

The robot was operating in a classroom to irradiate place, to tester, and see the influence with 13 points of microbial exposure, sampled in an area of 12.6 m<sup>2</sup>. The samples were analyzed by different time intervals in the laboratory, we used eq. (6) and we obtained the results, see Fig. 9a. The regression model eq. (6) allowed to measure the percentage of disinfection ( $Ef_i$ ) with the following test parameters: the wavelength used

shall be 253.7 nm, the exposure time was  $t_{min} = 2 s$  y  $t_{max} = 93s$ , the distance  $d_{min} = 2 mm$  and  $d_{max} = 231 mm$ , The exposure surface deltas where  $\delta_i = 0.25 m^2$ , separated into  $i = 12$  quadrants and  $j = 13$  samples randomly exposed in the corresponding quadrant. Then, the percentage of microbial elimination CFU/mL is determined, see **Error! Reference source not found.a**, **Error! Reference source not found.b** show the results of the  $i = 13$  samples and percentage of efficiency achieved.

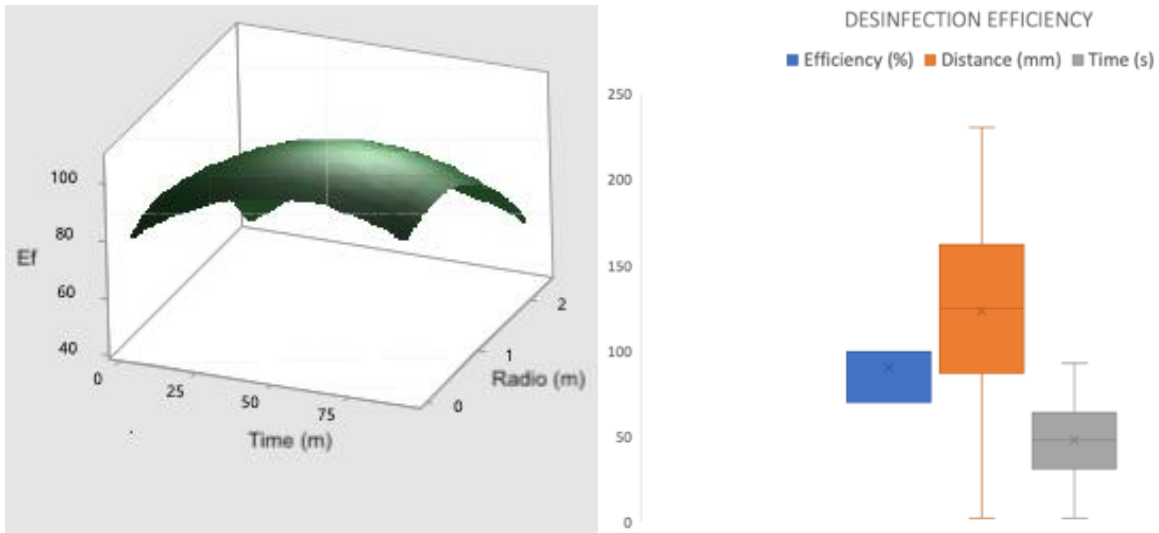


Fig. 9 a) Results of the regression model, b) Surface disinfection.

Taking into consideration the results obtained in [27] the irradiation dose to inactivate viruses and bacteria by UVC from 254 nm is  $3.7\mu J/cm^2$  to  $10.6\mu J/cm^2$ . In [28] recommended irradiation dose  $40\mu J/cm^2$ . This proposal achieves  $4.5382 W/m^2$ . The results of [29] using five lamps achieves a reduction of pathogens of 92% and 98% in 15 and 5 m. In [12] reports a performance of 84% in 0.9m linear. The present proposal using six lamps and achieves 95% in 14.763s in  $1m^2$ .

### 4.3. Calibration of the Olfactory System

To test the operation of the electronic nose with a high concentration of chemicals absorbed into the environment, we identify air quality patterns, and CO<sub>2</sub> and O<sub>3</sub> concentration level. First, we obtain the sensitivity of Sensors MQ-131 and MQ-135 (**Error! Reference source not found.**).

After, we calibrate the values by converting them to ppm. (Fig. 1) and we obtain the air sensitivity (Table 2).

Table 2. MQ-135 and MQ-131 air sensitivity.

<i>AIR(O<sub>3</sub>)</i>		<i>AIR (CO<sub>2</sub>)</i>	
X	Y	X	Y
4,9836	12,086	10,001	3,5807
5,9833	12,086	20,098	3,5807
6,9983	12,086	30,167	3,5807
8,0793	12,086	39,714	3,5807
8,9689	12,086	50,117	3,5807
9,9566	12,086	59,861	3,5807
19,892	12,086	69,414	3,5807
29,431	12,086	79,813	3,5807
40,264	12,086	89,47	3,5807
50,272	12,086	100,29	3,5807
58,8	12,086	10,001	3,5807
68,775	12,086	20,098	3,5807
79,398	12,086	30,167	3,5807
86,998	12,086	39,714	3,5807

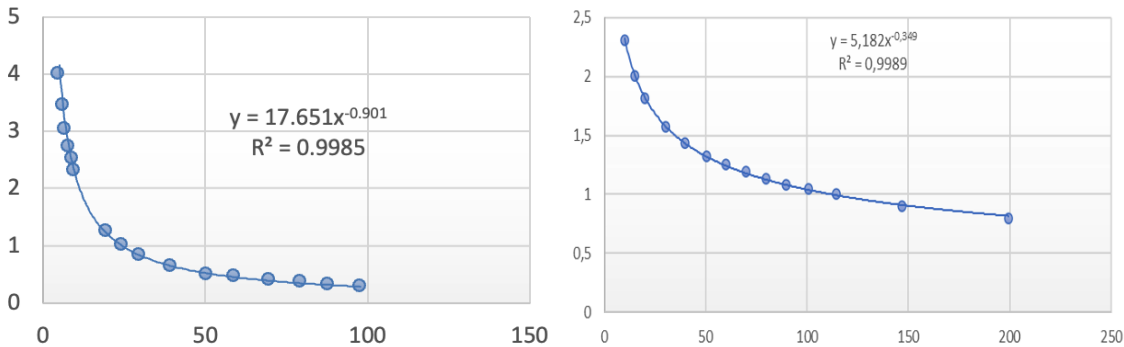


Fig. 10 O3 and CO2 sensitivity a) MQ-131, b) MQ-135

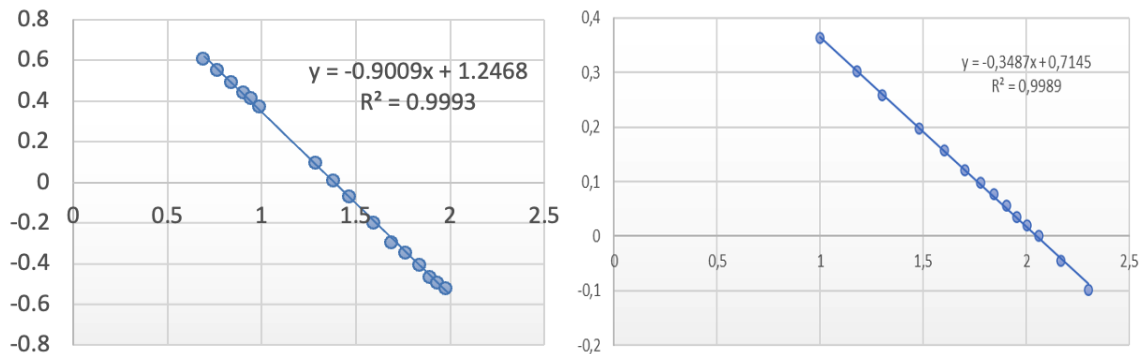


Fig. 1 O<sub>3</sub> and CO<sub>2</sub> calibration a) MQ-131, b) MQ-135

#### 4.4. Nebulizer system operation results

Once the olfactory system has been calibrated, the robot can start the disinfection process.

After that we need reduce the ozone level emitted by lamps. Then, to humidify a room of 12.5–18 m<sup>2</sup> and test the device, The nebulizer used 3 Piezoelectric placed in parallel, and H<sub>2</sub>O<sub>2</sub> solution. This setup allowed real-time monitoring of ozone concentration and other compounds in the air.

##### 4.4.1. Experimental Design

Two distinct tests were conducted to measure the efficiency of the nebulizer with the H<sub>2</sub>O<sub>2</sub> for reducing ozone concentration:

First Test:

Space Preparation: was closed to ensure a sealed environment. When the robot finishes your disinfection work, the olfactory system starts to measure the ozone concentration in enclosed spaces until a maximum concentration of 29.22 ppm was detected.

Waiting Time: When the space has the ozone concentration stabilize (about 3 minutes). Ozone Reduction: After 3 minutes, the space was opened to let the ozone escape. The ozone concentration decreased to 0.47 ppm within 15 seconds, see Fig. 12.

Second Test:

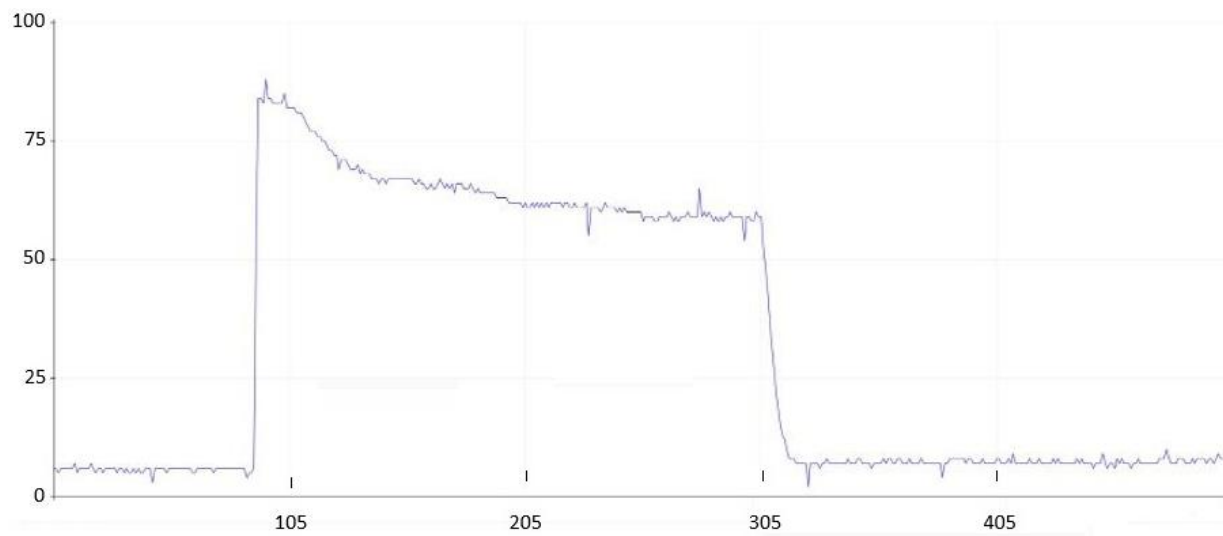


Fig. 12 Graphic with ambient ventilation

Space Preparation: was closed to ensure a sealed environment. When the robot finishes your disinfection work, the olfactory system starts the measure the ozone concentration in enclosed spaces until a maximum concentration of 29.22 ppm was detected. Waiting Time: When the space has the ozone concentration stabilize (about 3 minutes). Ozone Reduction: The ozone concentration dropped drastically to 0.05 ppm in just 3 seconds, see Fig. 13. By integrating the results from [19] and [20], this paper's proposal achieves 99.82% removal of indoor ozone

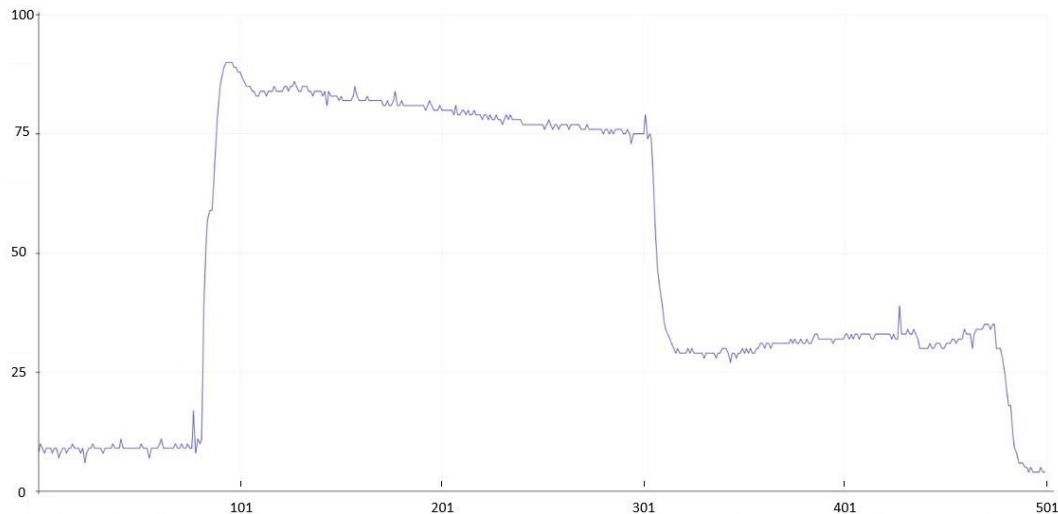


Fig. 13 Graphic with nebulizer system activate.

## 5 Conclusions and further work

This work highlights the importance of innovative solutions to improve indoor air quality. *Airborne Ozone Degradation, such as nebulization* is essential for neutralizing harmful ozone, ensuring safer and healthier environments. While UVC radiation is effective for microbial inactivation, its ozone-generating risks require integrated approaches that mitigate these effects.

Autonomous robotic platforms combining UVC lamps with hydrogen peroxide ( $H_2O_2$ ) nebulization address these challenges by enhancing disinfection efficiency, improving air quality, and minimizing environmental impact. Real-time monitoring through sensors like MQ-131 and MQ-135 ensures safe, resource-efficient operation.

The proposed platform provides a scalable, adaptable solution to current air purification limitations, contributing to public health resilience and sustainable urban development. This approach supports the creation of safer and more inclusive indoor environments.

The proposed solution showed good performance when we proof with microorganism like Salmonella. Therefore, this robot can sanitize surfaces, walls, floor, ceiling of corridors and closed rooms, covering and disinfecting the area at  $360^\circ$  of the robot in spaces of  $6.28 m^2$ , considering 6 central angles of  $60^\circ$  and an irradiated area of  $1.04 m^2$  per lamp. Therefore, to eliminate viruses and bacteria 99.9% is required on average  $4.5382 J/m^2$  of energy.

If the irradiated area is greater than  $6.28 m^2$ , the percentage of disinfection will be 70%. For short times (2-15s) and the influenced disinfection area is  $0.79-1m^2$ , 99.9% will be achieved. Finally, it is observed that the optimal time is  $14.76 s$  in an irradiated area of  $0.98-1.04 m^2$ , using  $4.5382 J/m^2$  of radiated energy of  $28.5 W$  of power in each lamp.

This data and the calibration of the MQ-131 and MQ-135 sensors will permit the disinfection system to automatically shut down avoiding contaminating the environment where the robot operates.

The data collected by the olfactory system were processed and analyzed to determine the efficiency of the H<sub>2</sub>O<sub>2</sub> compound for ozone elimination. The ozone reduction times between the two tests were compared to evaluate the impact of the nebulizer. The accuracy and reliability of the olfactory system ensured continuous and precise monitoring of ozone concentrations and other compounds throughout the experiment. The results obtained provide a clear evaluation of the effectiveness of the nebulized solution in mitigating ozone levels in enclosed environments.

The olfactory system and nebulizer integrated into the UVC Robot are considered functional elements, because it manages to capture gases from the environment, identify the level of pollution and clean the atmosphere to 99.82% in closed spaces without any ventilation.

To mitigate the degradation of the robot's materials due to prolonged exposure to ozone and hydrogen peroxide, resistant materials such as fluoropolymers and specialized coatings have been selected for critical components. These materials are designed to withstand the oxidative effects, ensuring the structural integrity of the robot over time. While this study primarily focuses on disinfection via UVC rays and nebulizer activation based on ozone measurements, the durability of key components is vital to guarantee long-term operational effectiveness.

The UVC lamps in this system have an estimated lifespan of approximately 10,000 hours, after which their intensity may decrease, thus reducing disinfection efficacy. To address this, we recommend a preventive maintenance schedule, including periodic intensity checks and prompt lamp replacement.

Because the ozone sensors will be exposed to varying ozone concentrations over time, they may experience sensitivity drift. Regular recalibration, recommended every 12 months, ensures accurate readings and reliable nebulizer activation. Furthermore, the nebulizer system, which operates with hydrogen peroxide, may experience nozzle clogging or wear. Scheduled inspections and cleaning are necessary to maintain its performance.

These considerations, combined with the platform's demonstrated efficiency in disinfection and air purification, affirm its potential as a robust and sustainable solution for improving indoor air quality in critical spaces. Thus, we will contribute to the 2030 Agenda for Sustainable Development in SDG3 and SDG11.

## Acknowledgements

This work was supported by TESE y LNC-IACD, in collaboration with COMECyT and TecNM. H. Sossa thanks the Instituto Politécnico Nacional and CONAHCyT for the support to undertake this investigation. The authors would like to express their gratitude to the researchers and students for their insightful contributions to attain this research.

## References

1. Benedick, R. E. (1996). Montreal Protocol on Substances that Deplete the Ozone Layer. *International Negotiation*, 1(2), 231–246.
2. Zhivov, A., Skistad, H., Mundt, E., & Posokhin, V. (2020). Principles of air and contaminant movement inside and around buildings. En *Industrial Ventilation Design Guidebook* (2nd ed., Vol. 1, pp. 245–370). Academic Press.
3. Galán Madruga, D. (2021). Implication of secondary atmospheric pollutants in the air quality: A case-study for ozone. En *Environmental Sustainability – Preparing for Tomorrow*. IntechOpen.
4. Baresel, C., Malmborg, J., & Sehlén, R. (2016). Removal of pharmaceutical residues using ozonation as intermediate process step at Linköping WWTP, Sweden. *Water Science & Technology*, 73(8), 2017–2024.
5. Gómez Castillo, M. A., Rivera Romero, C., Reátegui Ochoa, K., Mamani Zapana, E., & Silva-Jaimes, M. (2023). Ozone efficacy for the disinfection of ambulances used to transport patients during the COVID-19 pandemic in Peru. *International Journal of Environmental Research and Public Health*, 20(10), 5776.
6. Ruan, T., & Rim, D. (2019). Indoor air pollution in office buildings in mega-cities: Effects of filtration efficiency and outdoor air ventilation rates. *Sustainable Cities and Society*, 49, 101609.
7. Fong, W. C. G., Kadalayil, L., Lowther, S., Grevatt, S., & Potter, S. (2023). The efficacy of the Dyson air purifier on asthma control: A single-center, investigator-led, randomized, double-blind, placebo-controlled trial. *Annals of Allergy, Asthma & Immunology*, 130(22), 199–205.
8. Prasad, R., Uma, R., Kansal, A., Gupta, S., Kumar, P., & Saksena, S. (2002). Indoor air quality in an air-conditioned building in New Delhi and its relationship to ambient air quality. *Sage Journals Home*, 11(6).

9. Jing, L., & Wang, J. (2022). Study on indoor ozone removal by PRM under the influence of typical factors. *E3S Web of Conferences*, 356, 05037.
10. United Nations. (2023). *United Nations*. <https://unstats.un.org/sdgs/report/2020/>
11. Ishaan, M., Hao-Ya, H., Sharareh, T., Wenbin, L., & Sajad, S. (2023). UV disinfection robots: A review. *Robotics and Autonomous Systems*, 161, 104332.
12. Mikhailovskiy, N., Sedunin, A., Perminov, S., Kalinov, I., & Tsetserukou, D. (2021). UltraBot: Autonomous mobile robot for indoor UV-C disinfection with non-trivial shape of disinfection zone. En *26th IEEE International Conference on Emerging Technologies and Factory Automation (ETFA)*, Vasteras, Sweden.
13. Peña Suárez, J. M., Truffo, D., Bandera Cantalejo, J., González Muriano, M. D. C., Garcias Vacas, F., & Fernandez Hernández, F. (2022). Comparative study of purification technologies and their application to HVAC systems. *E3S Web of Conferences*, 343, 03005.
14. Chojer, H., Branco, P., Martins, F., Alvim Ferraz, C. A., & Sousa, S. (2024). Source identification and mitigation of indoor air pollution using monitoring data – Current trends. *Environmental Technology & Innovation*, 33, 103534, 1–21.
15. Malvestiti, J. A., & F. D., R. (2018). Disinfection of secondary effluents by O<sub>3</sub>, O<sub>3</sub>/H<sub>2</sub>O<sub>2</sub> and UV/H<sub>2</sub>O<sub>2</sub>: Influence of carbonate, nitrate, industrial contaminants and regrowth. *Journal of Environmental Chemical Engineering*, 6(1), 560–567.
16. Sauza, B., Dantas, R., & Cruz, A. (2014). Photochemical oxidation of municipal secondary effluents at low H<sub>2</sub>O<sub>2</sub> dosage: Study of hydroxyl radical scavenging and process performance. *Chemical Engineering Journal*, 237, 268–276.
17. Lidong, P., Chunyong, L., & Weidong, P. (2023). Research on the impact of indoor control quality monitoring based on Internet of Things. *IEEE Access*, 11, 139615–139627.
18. Zhibin, L., Guangwen, W., Liang, Z., & Guangfei, Y. (2021). Multi-points indoor air quality monitoring based on Internet of Things. *IEEE Access*, 9, 70479–70492.
19. Ramasubramanian, P. (2022). *Effectiveness of air pollution mitigation systems: Transport, transformation, and control of ozone in the indoor environment* [En línea]. Disponible en: [https://pdxscholar.library.pdx.edu/open\\_access\\_etds/6059/](https://pdxscholar.library.pdx.edu/open_access_etds/6059/)
20. Martínez Vimbert, R., Arañó Loyo, M., & Custodio Sánchez, J. D. (2020). Evidence of OH• radicals disinfecting indoor air and surfaces in a harmless for humans method. *International Journal of Engineering Research*, 6(4), 26–38.
21. Rossel Bernedo, L. J., Rossel Bernedo, L. A., Zapana Quispe, R. R., & otros. (2020). Radiation ultraviolet-C for bacterial disinfection (total and thermotolerant coliforms) in the water treatment. *Revista de Investigaciones Altoandinas*, 22(1).
22. Stawicki, S. P. (2020). Could tracheo-bronchial ultraviolet C irradiation be a valuable adjunct in the management of severe COVID-19 pulmonary infections? *International Journal of Academic Medicine*, 6(2), 156–158.
23. Yamano, N., Kunisada, M., & Kaidzu, S. (2020). Long-term effects of 222-nm ultraviolet radiation C sterilizing lamps on mice susceptible to ultraviolet radiation. *Journal of Photochemistry and Photobiology*, 96(4).
24. ASHRAE. (2019). Ultraviolet air and surface treatment. En *ASHRAE Handbook: Heating, Ventilating, and Air-Conditioning Applications* (pp. 1–17). ELSEVIER.
25. Kowalski, W. J., Walsh, T. J., & Petraitis, V. (2020). *COVID-19 Coronavirus Ultraviolet Susceptibility*. PurpleSun.
26. Carvajal, G., Branch, A., Michel, P., & Sisson, S. A. (2017). Robust evaluation of performance monitoring options for ozone disinfection in water recycling using Bayesian analysis. *Water Research*, 124, 605–617.
27. Heßling, M., Hönes, K., Vatter, P., & Lingenfelder, C. (2020). Ultraviolet irradiation doses for coronavirus inactivation – Review and analysis of coronavirus photoinactivation studies. *GMS Hygiene and Infection Control*, 2020.
28. Mankar, V., DhengreMedical, A., Agashe, N., Rodge, H., & Hari Chandi, D. (2022). Ultraviolet irradiation doses for coronavirus inactivation: Review and analysis of coronavirus photo inactivation studies. *International Journal of Health Sciences*, 6(S2), 466–472.
29. Eadie, E., Hiwar, W., Fletcher, L., & Tidswell, E. (2022). Far-UVC (222 nm) efficiently inactivates an airborne pathogen in a room-sized chamber.